MECHANICAL PROPERTIES AND FRACTURE SURFACE MORPHOLOGY OF EN AW 2024 ALUMINIUM ALLOY PREPARED BY ECAP

Fujda M.[1], Kvačkaj T.[2], Vojtko M.[1], Milkovič O.[1]
[1]Department of Materials Science, Faculty of Metallurgy, Technical University of Košice, Slovakia, e-mail: Martin.Fujda@tuke.sk
[2]Department of Metals Forming, Faculty of Metallurgy, Technical University of Košice, Slovakia, e-mail: Tibor.Kvackaj@tuke.sk

MECHANICKÉ VLASTNOSTI A MORFOLÓGIA LOMOVÝCH POVRCHOV HLINÍKOVEJ ZLIATINY EN AW 2024 PRIPRAVENEJ PROCESOM ECAP

Fujda M.[1], Kvačkaj T.[2], Vojtko M.[1], Milkovič O.[1]
[1]Katedra náuky o materiáloch, Hutnícka fakulta, Technická univerzita v Košiciach, Slovenská republika, e-mail: Martin.Fujda@tuke.sk
[2]Katedra tvárnenia kovov, Hutnícka fakulta, Technická univerzita v Košiciach, Slovenská republika, e-mail: Tibor.Kvackaj@tuke.sk

Abstrakt

V práci boli porovnané mechanické vlastnosti, mikroštruktúra a morfológia lomových povrchov tepelne spracovaných (rozpúšťacie žíhanie pri teplote 520°C + kalenie; žíhanie pri teplote 400°C + pomalé ochladzovanie), intenzívne plasticky deformovaných (ECAP), ECAPovaných a vystarnutých (prirodzené a umelé starnutie aplikované po ECAPe kaleného stavu) stavov Al-zliatiny EN AW 2024 s charakteristikami priemyselne produkovaných tyčí tejto zliatiny v stave T3 (východzí stav). Tepelne spracované stavy zliatiny boli intenzívne plasticky deformované technológiou ECAP pri teplote okolia. Jeden ECAP prechod kaleného stavu zliatiny vyvolal nerovnomernú distribúciu plastickej deformácie v objeme ECAPovaných vzoriek, ktorá sa prejavila vznikom sklzových pásov s rozdielnou intenzitou deformácie v štruktúre zliatiny. Homogénna distribúcia plastickej deformácie v objeme zliatiny je výsledkom dvoch ECAP prechodov žíhaného stavu zliatiny. V intenzívne plasticky deformovanej mikroštruktúre ECAPovaných stavov boli pozorované ultrajemné subzrná s vysokou dislokačnou hustotou. Výsledkom ECAPu je značné deformačné spevnenie zliatiny, ktoré sa prejavilo vo zvýšení pevnostných vlastností, avšak v poklese plasticity a vrubovej húževnatosti analyzovanej zliatiny. Nahradenie post-ECAPového prirodzeného starnutia zliatiny umelým viedlo k nepatrnému zlepšeniu plasticity, pevnosti a vrubovej húževnatosti ECAPovanej zliatiny. Vzorky východzieho stavu a tepelne spracovaných stavov zliatiny boli pri skúške ťahom a skúške rázom v ohybe porušené tvárnym lomom a ich lomové povrchy majú jamkovú morfológiu. Stupňovitý charakter lomových povrchov intenzívne plasticky deformovaných stavov je výsledkom deformácie a lomového procesu v šmykových rovinách. Vzorky stavov zliatiny ECAPovaných po kalení vykazovali zmiešanú morfológiu lomových povrchov pozostávajúcu z faziet transkryštalického štiepenia v okolí nepravidelných viacfázových intermetalických častíc a jamiek transkryštalického tvárneho porušenia formovaných na rozhraniach disperzných častíc so zvýšeným obsahom Mn a matrice. V prípade vzoriek stavu ECAPovaného po žíhaní mali lomové povrchy jamkovú morfológiu, ktorá je výsledkom vzniku mikrodutín na rozhraniach intermetalických častíc a matrice, príp. prasknutím nepravidelných

viacfázových intermetalických častíc a ich následnej koalescencie vyvolanej deformáciou a lomovým procesom v šmykovej rovine.

Abstract

The mechanical properties, microstructure and fracture morphology of EN AW 2024 aluminium alloy subjected to heat treatment (solution annealing at 520°C + water quenching or annealing at 400°C + slow cooling), severe plastic deformation (ECAP) and post-ECAP treatment (natural or artificial ageing after ECAP of quenched state) are compared with those of the industrially processed alloy rods in T3 temper (initial state). The heat treated states of alloy were severely deformed at ambient temperature by equal channel angular pressing (ECAP). The ECAP pass of quenched alloy state caused a non-uniform plastic deformation throughout the ECAPed specimens and slip bands with different amount of deformation in microstructure were formed. On the contrary, homogeneous severe plastic deformation was obtained using the double ECAP of annealed alloy state. Formation of ultra-fine subgrains with high dislocation density in intensive deformed microstructure, high strain hardening of alloy and thus an improvement in strength, but degradation of the ductility and notch toughness of analyzed alloy was a result of severe plastic deformation in the ECAP die. Application of the post-ECAP artificial ageing instead of natural ageing slightly improved ductility, strength and notch toughness of ECAPed and aged alloy. Specimens of initial and heat treated alloy states were fractured in ductile manner during tensile or impact test and shows dimple morphology of their fracture surfaces. Fracture surfaces of ECAPed alloy states with a stage character were a result of deformation and fracture process in shear planes. Specimens of alloy states ECAPed after quenching showed a mixed morphology of fracture surfaces which consists of transgranular cleavage facets in the vicinity of irregular multiphase intermetallic particles and dimples of transgranular ductile fracture nucleated at matrix/Mn-rich phase particles interfaces. Specimens fracture surface of alloy states ECAPed after annealing had dimple morphology. It was a result of the voids nucleation at intermetallic particles/matrix interfaces or by irregular multiphase intermetallic particles cracking and its coalescence by deformation and fracture process on the shear plane.

Keywords: EN AW 2024 aluminium alloy, equal channel angular pressing (ECAP), ultra-fine grain microstructure, mechanical properties, fracture morphology

1. Introduction

EN AW 2024 aluminium alloy is widely used as AlCuMgMn alloy in miscellaneous applications on the score of its excellent strength vs. density ratio, formability and corrosion resistance [1-3]. Alloys of this type have been considered as a substitute of steel in the transportation industry. Several technical compositions are standardized and new alloys of this type with lower content of impurities are developed [4, 5].

EN AW 2024 alloy is age-hardenable alloy which is subjected to a solution treatment, quenching, and a natural or artificial ageing treatment in order to obtain the optimum combination of mechanical properties. The coarse intermetallic phase particles present in structure of this alloy type are responsible for the low fracture resistance [6]. The formation of intermetallic particles results from the presence of impurities, e.g. Fe and Si, and excessive content of alloying elements such as Cu, Mg and Mn in this type of alloy. Therefore the

important requirement is to lower of the coarse intermetallic particles volume fraction in this type of alloys and in this manner to improve the fracture toughness and the plasticity of alloys [6 -10].

Equal channel angular pressing (ECAP) technique is very useful in improving strength of Al-based alloy through grain refinement to the submicron but also to nanometer level [11-17]. Severe plastic deformation by the ECAP process also increases markedly the density of lattice defects in the solid solution and thus can accelerated the precipitation process of strengthening particles during the post-ECAP ageing treatment applied for the age-hardenable aluminium alloy [15,18,19]. However, ultra-fine-grained age-hardenable alloys often exhibit low tensile ductility at room temperature. Therefore, it is important to obtain the ductility comparable to that of conventional coarse-grained age-hardenable Al-based alloys. Pre-ECAP solution treatment plus post-ECAP low temperature ageing treatment is also very effective in improving the strength of 2024 aluminium alloy [15]. In addition, special heat-treated 2024 aluminium alloy subjected to severe plastic deformation by ECAP procedure showed a superplastic forming capability [17].

However, only a few works dealt with deformation and fracture mechanism of ECAPed wrought Al-based alloys in detail were published [20-24]. Authors established a possible connection between mechanical properties and fracture behaviour of the ECAPed alloys. Under tensile load of samples, the fracture tends to proceed along the maximum shear stress plane. The shear fracture angles are usually ranged from 45° to 60°, which indicates that the shear fracture of ECAPed aluminium alloys is controlled by both shear and normal stresses [20, 21]. The elongated dimple fracture morphology was prevailing over the ductile tensile fracture surfaces. Microvoids nucleation and subsequent voids coalescence by strong shear deformation and fracture process on the shear plane formed the elongated dimples on fracture surface [22, 23].

The aim of the present work is to investigate the effect of heat treatment and severe plastic deformation by ECAP on microstructure, mechanical properties and fracture morphology of EN AW 2024 aluminium alloy.

2. Materials and experimental

The investigation has been carried out on the commercial aluminium alloy EN AW 2024 which chemical composition is indicated in Table 1. The rolled bar industrially processed in T3 temper was used like initial alloy state in a present investigation. Prior to deformation in an ECAP die, specimens of the initial alloy state were subjected to a heat treatment:

- solution annealing at 520°C (holding time: 2.5 h) + cooling to ambient temperature by water quenching (quenched state) – to dissolve GPB-zones, S''- and S'- Al_2CuMg phase particles into solid solution and to obtain supersaturated solid solution
- annealing at 400°C (holding time: 2.5h) + slow cooling (cooling rate: 100°C/h) to the ambient temperature (annealed state) – to obtain saturated solid solution and relatively coarse dispersive Al_2CuMg phase particles distributed homogeneously in solid solution

Table 1 Chemical composition (content in wt. %) of the investigated EN AW 2024 alloy

Cu	Mg	Mn	Fe	Si	Zn	Al
4.2	1.4	0.91	0.20	0.10	0.03	bal.

The quenched or annealed specimens were subjected to severe plastic deformation in an ECAP die having a channel intersection angle $\Phi = 90°$ and arc of curvature $\Psi = 37°$. The

ECAP of specimens of size ∅ 10 mm x 80 mm was attempted at ambient temperature following route C (a 180° rotation of the specimen between each pass) [25]. Severe cracking took place by shear mode during the second or third ECAP pass of quenched or annealed alloy state, respectively. Hence, after one ECAP pass the quenched specimen were subjected to natural or artificial ageing for 300h at 100°C. This artificial ageing time (300 h) was optimal to obtain the highest hardness of ECAPed alloy state during artificial ageing at 100°C [26].

Microstructure of the investigated alloy after quenching or annealing, deformation in the ECAP die and in some case after post-ECAP ageing treatment were analyzed in the central zone of the specimen's cross-section using a transmission electron microscopy (TEM). The foils for TEM were prepared using common metallographic methods and finally thinned in a solution of 25%HNO_3 and 75%CH_3OH at a temperature -30°C. TEM was conducted at an accelerating voltage of 200kV.

The influence of the applied heat treatment, severe plastic deformation by ECAP process and eventually post-ECAP natural or artificial ageing on the mechanical properties of the analyzed alloy was evaluated by a tensile test and an impact test. The tensile test (deformation rate 2.5 x 10^{-4} s^{-1}) was carried out on short specimens (Fig. 1) made from ECAP processed billet by machining along the longitudinal direction. Subsequently, characteristics of the strength (yield stress: $R_{p0.2}$; ultimate tensile strength: R_m), elongation (A_2) and reduction in area (Z) were determined. Impact test samples were also made from ECAP processed billet by machining along the longitudinal direction. The size of the test pieces was 8 mm x 4 mm in cross-section and 55 mm in length, with a V-notch 1 mm in depth (Fig. 2). Charpy impact test machine was used for measuring the absorbed energy of the samples as the notch toughness (KCV) at ambient temperature. Fracture surfaces morphology of analyzed alloy states after tensile and impact test was investigated using a scanning electron microscopy (SEM).

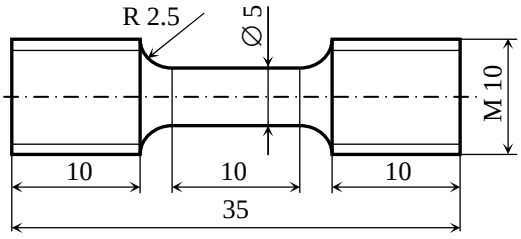

Fig.1 The geometry and dimensions (in mm) of short specimen for tensile test

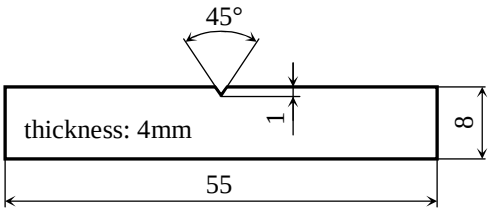

Fig.2 The geometry and dimensions (in mm) of short specimen for impact test

3. Results and discussion

3.1 Microstructure

Coarse irregular intermetallic particles, undissolved Al_2CuMg particles and fine dispersive Mn-rich particles were observed in microstructure of alloy initial state [27, 28]. Character of solid solution grains is equiaxed (grain size: ~3 μm) with relatively high dislocation density, as shown in Fig. 3a. Figs. 3b and 3c show the equiaxed grains and subgrains with low dislocation density found in microstructure of quenched or annealed alloy state, respectively. The relatively coarse dispersive rod-like Al_2CuMg phase particles distributed mainly in the boundaries of solid solution grain and subgrain were observed in annealed alloy state (Fig. 3c). No growth or a moderate growth of solid solution equiaxed grains was found after annealing at 400°C (grain size: 3.5 μm) or after solution annealing at 520°C (grain size: 6.5 μm) applied for

alloy initial state, respectively. Solid solution grains growth was prevented by grain boundary pinning effect of fine dispersive particles. These fine (size: 30 - 120 nm) dispersive particles documented in Fig. 3 were identified as Mn-rich phase particles (probably $Al_{20}Cu_2Mn_3$ phase particles) and they were distributed homogeneously throughout the alloy states. In commercial age-hardened aluminium alloys Mn is usually added to form dispersive particles, which aid in the matrix grain size control during applied heat treatment [7, 10, 29 -32]. Character of the coarse irregular particles (average size: 7 μm) which were present in alloy initial state was not markedly influenced by applied heat treatment and severe plastic deformation in ECAP die. These particles are intermetallic multiphase particles with high content of Al, Fe, Mn and Cu [26 -28].

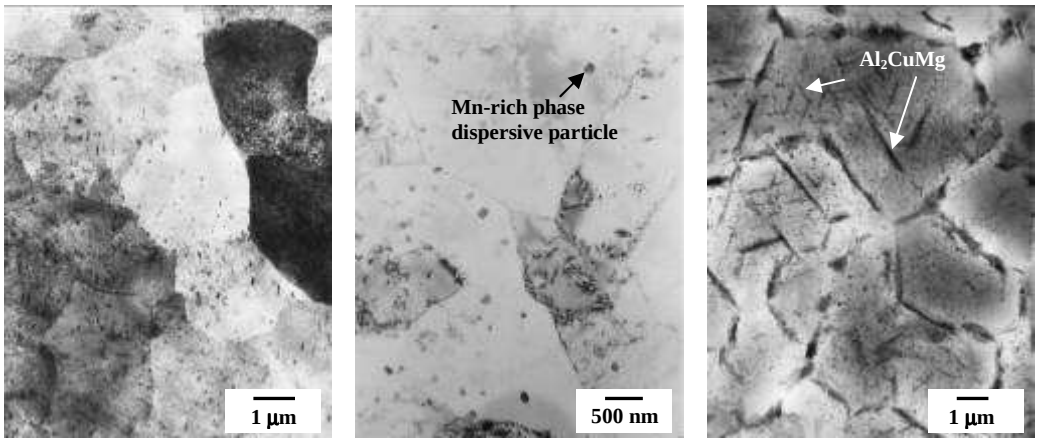

a) b) c)

Fig.3 Microstructure of unECAPed alloy states; TEM a) initial state; b) quenched state; c) annealed state

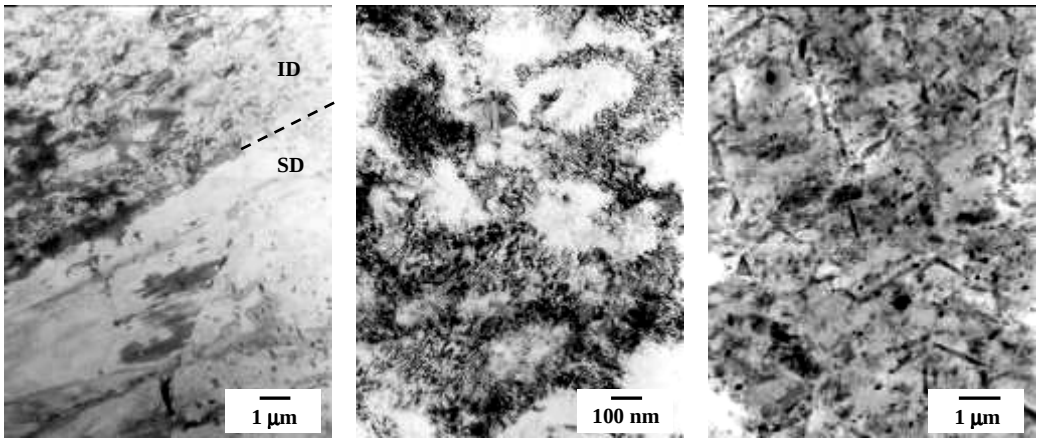

a) b) c)

Fig.4 Microstructure of ECAPed alloy states; TEM

a) quenched + ECAPed + naturally aged; ID – the intensively deformed region, SD – the slightly deformed region

b) quenched + ECAPed + artificially aged; detail of the intensively deformed region

c) annealed + ECAPed

Heterogeneous microstructure of severely deformed (ECAPed) alloy after quenching was characterized using a light microscopy in the work [26]. Formation of deformation bands with very different amount of deformation indicated the non-uniform deformation across the cross-section of ECAPed specimens. The character of severely deformed heterogeneous structure was appreciated more exactly using the transmission electron microscopy (TEM). Fig. 4a shows TEM micrograph illustrating the analyzed alloy microstructure in the vicinity of interface (dash line) between intensively deformed (ID) and slightly deformed region (SD) observed for alloy state quenched, ECAPed and subsequently naturally aged. Many ultra-fine subgrains (subgrain size: ~180 nm) with very high dislocation density and dislocation cells created by slip during ECAP process were observed in the intensively deformed (ID) region of microstructure. A similar morphology of deformed microstructure with a very high density of dislocations accumulated and stored in the subgrains and in subgrain's boundaries was observed after the 80% cryo-rolling strain of the solution annealed and subsequently quenched 2024 aluminium alloy [33]. On the contrary, a dislocation density in the slightly deformed (SD) region of microstructure was considerably smaller. In this region (SD) of microstructure, some tangles of dislocations created by slip were accumulated near the boundaries of grains formed during the pre-ECAP heat treatment of analyzed alloy, which is shown in Fig. 4a.

A slight dislocation recovery in the ultra-fine subgrains (subgrain size: ~180 nm) and in the dislocation cells, which is manifested by dislocations arrangement (polygonization) shown in Fig. 4b was observed in the intensively deformed regions (ID) after artificial ageing (100°C/300h) of the ECAPed alloy. An analysis by a high resolution transmission electron microscopy should be carried out to evaluate formation of the GPB zones and the metastable Al_2CuMg phase (S'', S') particles during applied ageing treatments after ECAP of analyzed alloy.

Fig. 4c shows a homogeneously deformed microstructure with a high density of dislocations accumulated and stored in the subgrains (subgrain size: ~350 nm), which was observed after ECAP of annealed alloy state. In addition, fragmentation of rod-like Al_2CuMg phase particles took place. The average subgrains size measured for this state is higher in comparison with subgrains size observed in intensive deformed region for the alloy states ECAPed after quenching. It was due to different solid solution character and mechanical properties of alloy prepared by solution annealing and water quenching or annealing and slow cooling before ECAP.

3.2 Tensile test

The stress-strain curves of the initial, unECAPed (quenched or annealed) and ECAPed analyzed alloy states are shown in Figs. 5 and 6. Values of yield stress ($R_{p0.2}$), ultimate tensile strength (R_m), elongation (A_2) and reduction in area (Z) of the analyzed alloy states are summarized in Table 2. Moderate value of the yield stress and relatively high tensile ductility was characteristic for the recrystallized equiaxed microstructure of the heat treated (quenched or annealed) analyzed alloy. The significant strengthening of heat treated alloy states was obtained by only single or double ECAP. Yield stress of the ECAPed states of alloy is higher by ~ 120 % than that obtained for the relevant heat treated alloy states (annealed or quenched), while tensile elongation of alloy, on the other hand, was lower more than half for severely deformed alloy states. A similar change of strength and ductility of 2024 aluminium alloy after the single ECAP was found by Kim et al. [15]. The observed decrease in tensile ductility, the high strength and the high value of $R_{p0.2}/R_m$ ratio (~0.95) of the ECAPed state indicated that the increase in the

strength is first of all a consequence of the expressive strain hardening of the solid solution by the ECAP process. Therefore the ECAPed alloy has a relatively small strain hardening ability after yielding during the tensile test.

Of course, an assumed formation of the GPB-zones and metastable phases (S″, S′) particles during applied post-ECAP ageing treatment contributed to the strength of alloy state ECAPed after quenching. When post-ECAP natural ageing was replaced by artificial ageing at 100°C, further increase in $R_{p0.2}$ and R_m of the ECAPed alloy was found (Fig. 5, Table 2). This artificial ageing treatment is also effective in a slight improving the ECAPed alloy tensile ductility in consequence of the partial dislocation recovery in the intensive deformed bands of the ECAPed alloy microstructure. Kim et al. [15] achieved the similar increase of the strength and ductility of the ECAPed 2024 aluminium alloy by application of artificial ageing treatment at 100°C because the hardening effect by ageing dominates the softening effect by microstructure recovery and relaxation of internal stress. Hence, the ECAP and post-ECAP ageing applied for investigated EN AW 2024 aluminium alloy allowed to obtain the higher strength than the commonly used industrial processing (initial state-Table 2).

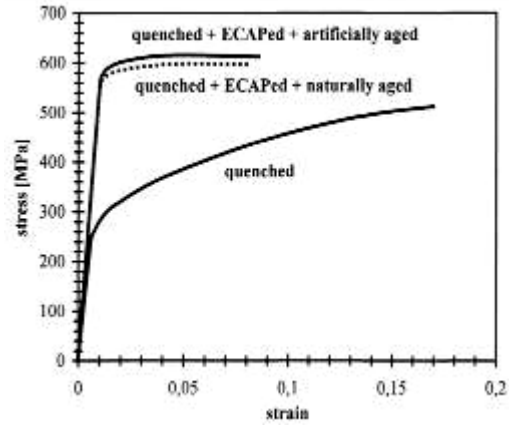

Fig.5 Tensile stress-strain curves for the quenched and ECAPed states of analyzed alloy

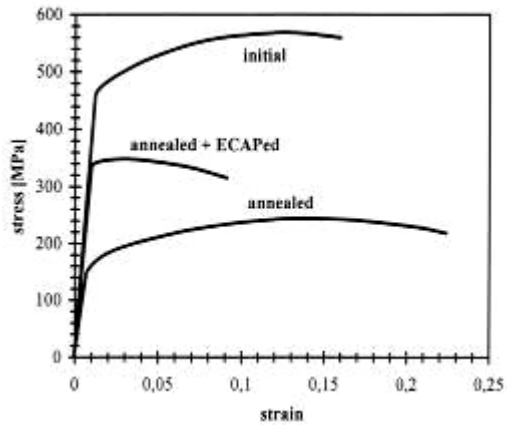

Fig.6 Tensile stress-strain curves for the initial, annealed and ECAPed states of analyzed alloy

Table 2 Mechanical properties of analyzed alloy states

alloy state	**$R_{p0.2}$ [MPa]**	**R_m [MPa]**	**A_2 [%]**	**Z [%]**	**KCV [J.cm^{-2}]**
initial	464	571	14.5	17.2	17.1
annealed	153	247	21.3	30.3	23.8
quenched	259	510	16.1	12.3	37.3
annealed + ECAPed	339	351	8.3	16.4	10.7
quenched + ECAPed + naturally aged	561	598	6.9	7.8	9.9
quenched + ECAPed + artificially aged	573	615	7.5	10.1	10.1

3.3 Impact test

Values of notch toughness (KCV) of alloy states are summarized in Table 2. Notch toughness of the heat treated (quenched or annealed) specimens of alloy is relatively high. Impact testing of these specimens was carried out immediately after the heat treatment. In this case, the recovery and/or recrystallization of the alloy took place during annealing treatment and

the precipitation of the strengthening phases (GPB – zones, S", S') before impact testing of quenched state can be ignored.

The notch toughness measured for ECAPed alloy states was decreased markedly reaching ~10 J.cm^{-2}. These values are more then 2 or 3 times lower than values of notch toughness obtained for annealed (23.8 J.cm^{-2}) or quenched (37.3 J.cm^{-2}) alloy state, respectively. The reason of this toughness loss is first of all the heterogeneous and/or intensive strain hardening of analyzed alloy during the ECAP. Therefore, the initial state with lower strain hardening showed slightly higher notch toughness then ECAPed ones. Of course, the coarse irregular multiphase intermetallic particles, Al_2CuMg particles, dispersive Mn-rich phase particles and the assumed precipitation of strengthening phases during post-ECAP ageing of analyzed alloy have also some detrimental effect on the notch toughness of the ECAPed EN AW 2024 aluminium alloy.

3.4 Fracture morphology

Figs. 7 and 8 show typical morphology of fracture surface observed for the heat treated (quenched, annealed) analyzed alloy states. These specimens were fractured in ductile manner during tensile or Charpy impact test. Their fracture surfaces consisted of numerous dimples with various sizes over the entire surface. The dimples were a result of the microvoids nucleation at intermetallic particles/matrix interfaces or by irregular multiphase particles cracking and its coalescence in the shear planes. The average dimple size listed in Table 3 is different for individual unECAPed alloy states because various intermetallic phase particles as coarse irregular multiphase particles, Al_2CuMg phase particles and eventually dispersive Mn-rich phase particles take a dominant role in the fracture process during tensile and impact test.

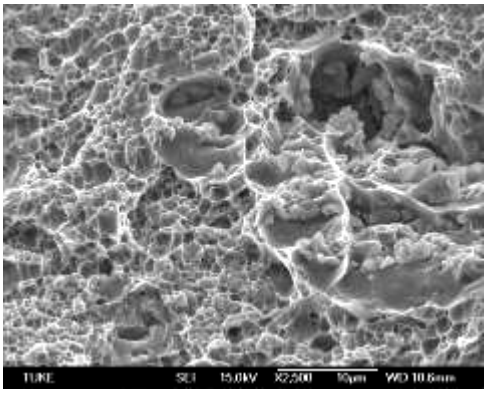

Fig.7 Fracture surface morphology of quenched alloy state; SEM, tensile test

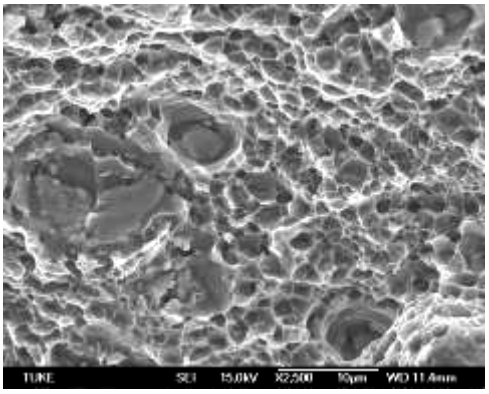

Fig.8 Fracture surface morphology of annealed alloy state; SEM, impact test

Figs. 9 and 10 show typical fracture surface morphology of the ECAPed alloy states. Fracture surfaces of ECAPed alloy states had a stage character and they were a result of deformation and fracture process in shear planes, which is the evidence that the plasticity of ECAPed alloy states decreased as a result of strain hardening [20]. Specimens of alloy states ECAPed after quenching showed a mixed mode of fracture. Transgranular cleavage in the irregular multiphase particles vicinity and very fine dimples of transgranular ductile fracture

nucleated at matrix/dispersive Mn-rich phase particles interfaces coexisted on these fracture surfaces, as shown in Fig. 9. Specimens of alloy which was ECAPed after annealing were fractured in ductile manner and fracture surface of alloy states ECAPed after annealing had dimple morphology. Fracture mode of these specimens consists of numerous dimples, which nucleated mainly at matrix/rod-like Al_2CuMg particles interface and by irregular multicomponent phase particle cracking. The average dimple size was smaller for ECAPed alloy states in comparing with that observed for unECAPed ones (Table 3). In addition, the increased area fraction of very fine dimples (size: 0.45 μm) nucleated at interfaces of dispersive Mn-rich phase particles/matrix was observed on fracture surfaces of ECAPed alloy states in comparison with fracture surfaces of initial and heat treated states. Even though intermetallic phase particles take again a dominant role in the fracture process during tensile and impact test of ECAPed alloy states, the decrease in the dimple size can be explained by microstructure refinement as well as strain hardening and the fragmentation of particles caused by ECAP [20, 34].

Table 3 Average size of dimples nucleated by particle cracking and/or at particles/matrix interfaces which were observed on fracture surfaces of initial and heat treated (quenched, annealed) and ECAPed alloy states

alloy state	**irregular multiphase particles**	**rod-like Al_2CuMg phase particles**	**dispersive Mn-rich phase particles**
initial	9 μm*		0.55 μm
annealed	9 μm	2.5 μm	—
quenched	12.5 μm	—	0.75 μm
annealed + ECAPed	8.5 μm	2 μm	0.45 μm
quenched + ECAPed + naturally aged	no dimples	—	0.45 μm
quenched + ECAPed + artificially aged	no dimples	—	0.45 μm

* irregular multiphase particles and undissolved Al_2CuMg phase particles

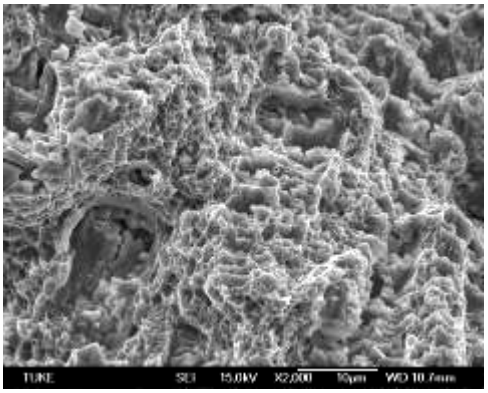

Fig.9 Fracture surface morphology of quenched, ECAPed and naturally aged alloy state, SEM, tensile test

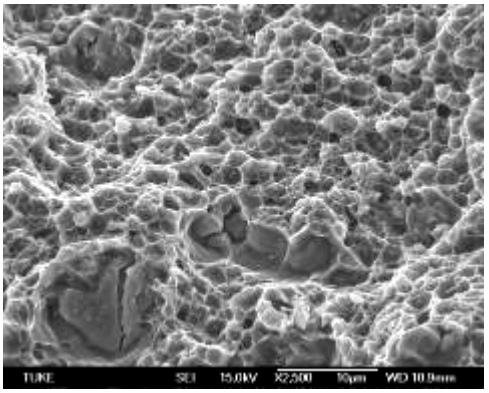

Fig.10 Fracture surface morphology of alloy ECAPed after annealing; SEM, impact test

4. Conclusion

The single ECAP of the quenched EN AW 2024 aluminium alloy induced the non-uniform plastic deformation throughout the ECAPed specimens. In the intensively deformed region of microstructure dislocation cells and many ultra-fine subgrains with very high dislocation density were observed. Homogeneously deformed microstructure with a high density of dislocations accumulated and stored in the subgrains and fragmentation of rod-like Al_2CuMg phase particles was characteristic for alloy state ECAPed after annealing.

The significant strengthening, on the other hand, the decrease in tensile ductility and notch toughness of ECAPed alloy states resulted from the intensive strain hardening of the solid solution by the ECAP process.

Fracture morphology of ECAPed alloy specimens consisted of transgranular cleavage facets in irregular multiphase particles vicinity and/or transgranular ductile fracture with dimples nucleated at interfaces of matrix/intermetallic particles. The smaller average dimple size was found on fracture surfaces of ECAPed alloy states in comparing with obtained results for unECAPed ones. Even though various intermetallic phase particles take a dominant role in the fracture process during tensile and impact test, the decrease in the dimple size can be explained by microstructure refinement as well as matrix strain hardening caused by ECAP.

Acknowledgment

This work was supported by the Scientific Grant Agency of Slovak republic as grant project No. 1/3217/06 and by the Slovak Research and Development Agency as project APVV-20-027205.

Literature

[1] Polmear I.J.: The Metallurgy of the Light Metals, Light Alloys, Arnold, 1995, London.
[2] Mondolfo L.F.: Aluminium Alloys: Structure and properties, 1976, Butterworth, London.
[3] Spigarelli S., Cabibbo M., Evangelista E., Bidulská J.: Journal of Materials Science, vol. 38, 2003, p. 81-88.
[4] Ratchev P., Verlinden B., De Smet P., Van Houtte, P.: Materials Transactions, JIM, vol. 40, 1999, p. 34.
[5] http://www.aluminum.org/
[6] Wang S. C., Starink M. J.: Acta Materialia, vol. 55, 2007, p. 933.
[7] Garrett G.G., Knott J.F.: Metallurgical Transaction, vol. A9, 1978, p. 1187.
[8] Gang Liu, Jun Sun, Ce-Wen Nan, Kang-Hua Chen: Acta Materialia, vol. 53, 2005, p. 3459.
[9] Liu G., Zhang G.J., Ding X.D., Sun J., Chen K.H.: Materials Science and Technology, vol. 19, 2003, p. 887.
[10] Hahn G. T., Rosenfield A. R.: Metallurgical Transaction. vol. A6, 1975, p. 653.
[11] Valiev R.Z., Estrin Y., Horita Z., Langdon T. G., Zehetbauer M., Zhu Y.T.: JOM, vol. 58, 2003, p. 33.
[12] Lowe T.C., Valiev R.Z. (Eds.): Investigations and Applications of Severe Plastic Deformation, Kluwer, 2000, Dordrecht, the Netherlands.
[13] Zehetbauer M.J., Valiev, R.Z. (Eds.): Nanomaterials by Severe Plastic Deformation, Wiley – VCH, 2004, Weinheim, Germany.
[14] Horita Z. (Ed.): Nanomaterials by Severe Plastic Deformation, Trans Tech Publications, 2005, Uetikon – Zurich, Switzerland.
[15] Kim W.J., Chung C.S., Ma D.S., Hong S.I., Kim H.K.: Scripta Materialia, vol. 49, 2003, p. 333.
[16] Lee S., Furukawa M., Horita Z., Langdon T.G.: Materials Science and Engineering, vol. A342, 2003, p. 294.
[17] Horita Z., Fujinami T., Nemoto M., Langdon T.G.: Journal of Materials Processing Technology, vol. 117, 2001, p. 288.
[18] Murashkin M.Y., Markushev M.V., Ivanisenko Y.V., Valiev R.Z.: Solid State Phenomena, vol. 114, 2001, p. 91.

[19] Jong Kap Kim, Woo Jin Kima: Solid State Phenomena, vols. 124 -126, 2007, p. 1437.
[20] Fang D. R., Duan Q. Q., Zhao N. Q., Li J. J., Wu S. D., Zhang Z. F.: Materials Science and Engineering, vol. A459, 2007, p. 137.
[21] Fang D. R., Zhang Z. F., Wu S. D., Huang C. X., Zhang H., Zhao N. Q., Li J. J.: Materials Science and Engineering, vol. A426, 2006, p. 305.
[22] Si-Young Chang, Byong-Du Ahn, Sung-Kil Hong, Shigeharu Kamado, Yo Kojima, Dong Hyuk Shin: Journal of Alloys and Compounds, vol. 386, 2005, p. 197.
[23] Segal V. M.: Materials Science and Engineering, vol. A406, 2005, p. 205.
[24] Yang Gon Kim, Byoungchul Hwang, Sunghak Lee, Woo Gyeom Kim, Dong Hyuk Shin: Metallurgical and Materials Transactions, vol. A36, 2005, p. 2947.
[25] Iwahashi Y., Wang J., Horita Z., Nemoto M., Langdon, T.G.: Scripta Materialia, vol. 35, 1996, p. 143.
[26] Fujda M., Kvačkaj T., Milkovič O., Longauerová M.: Journal of Metals, Materials and Minerals, vol.18, No. 2, accepted for publishing
[27] Fujda M., Rusňáková L.: Acta Metallurgica Slovaca. vol. 13, SI 1, 2007, p. 644
[28] Fujda M., Mišičko R., Rusňáková L., Sojko M.: Journal of Metals, Materials and Minerals, vol. 17, No. 1, 2007, p. 35
[29] Vander Voort G.F. (Ed): Metallography and Microstructures, ASM Handbook, vol. 9**,** ASM International, 2004, Ohio-USA, 1184 p.
[30] C. Zener quoted in C.S. Smith, Trans, AIME, 175, 1948, p. 15.
[31] Anne Lise Dons: Journal of Light Metals, vol. 1, 2001, p. 133.
[32] Rios P.R., Fonseca G.S.: Scripta Materialia, vol. 50, 2004, p. 1373.
[33] Cheng S., Zhao Y.H., Zhu Y.T., Ma E.: Acta Materialia, vol. 55, 2007, p. 5822.
[34] Young Gun Ko, Dong Hyuk Shin, Kyung-Tae Park, Chong Soo Lee: Scripta Materialia, vol. 54, 2006, p. 1785.